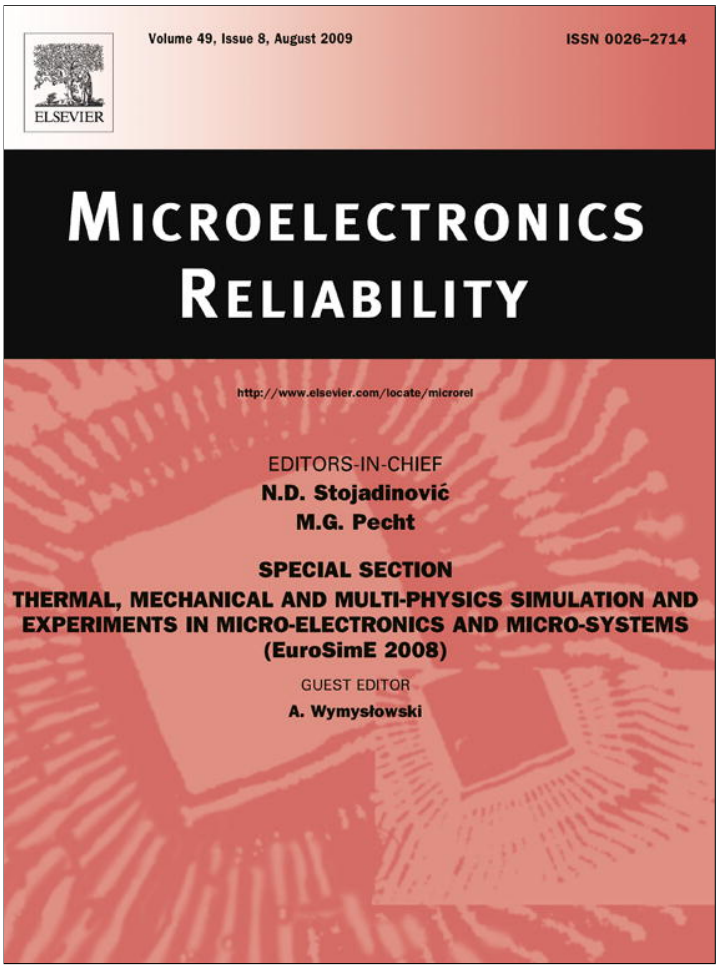

Microelectronics Reliability 49 (2009) 861–871

Contents lists available at ScienceDirect

Microelectronics Reliability

journal homepage: www.elsevier.com/locate/microrel

Experimental investigations and model study of moisture behaviors in polymeric materials

X.J. Fan [a,c,*], S.W.R. Lee [b], Q. Han [c]

[a] Department of Mechanical Engineering, P.O. Box 10028, Lamar University, Beaumont, TX 77710, USA
[b] Department of Mechanical Engineering, Hong Kong University of Science and Technology, Clear Water Bay, Kowloon, Hong Kong
[c] Department of Engineering Mechanics, South China University of Technology, Guangzhou 510640, China

ARTICLE INFO

Article history:
Received 13 October 2008
Received in revised form 28 February 2009
Available online 23 April 2009

ABSTRACT

In the present study, several experiments were performed to investigate the fundamental characteristics of moisture behaviors in various polymer materials and the interactions of water molecules with polymer matrix. Moisture weight gain tests were performed with different packaging materials. Both Fickian and non-Fickian diffusion behaviors were observed. The mold compound under investigation showed stronger non-Fickian absorption kinetics than the underfill. For most polymer materials in electronics packaging, saturated moisture concentration does not depend on temperature but relative humidity only as long as the temperature is far below the glass transition temperature. However, the saturated moisture content may increase significantly with temperature when the temperature is across the glass transition temperature. There are two distinct diffusion mechanisms involved in the transport of moisture: transfer across surface and transfer through bulk. Water sorption appears to be different from moisture sorption. Hydrophobic film can prevent water liquid molecules from penetrating through the surface. However, this has never been effective for the water vapor transmission through hydrophobic materials. Further in this study, mercury intrusion method was introduced to characterize the pore size and porosity of various materials. For most polymer materials, the free volume or pore sizes are in nano-meter range though the free volume fraction is usually in the range of 1% to 5%. Significant voiding can be developed at reflow process for soft films. An approximate estimation of free volume fraction using weight gain data was proposed. Furthermore, the moiré interferometry technique was employed to study the aging effect of hygroscopic swelling. It was found that hygroscopic swelling is coupled with viscoelastic deformation. At last the mathematical descriptions of moisture phase transition with temperature and the governing equations for a deforming polymer with moisture effect are presented in this paper.

1. Introduction

Many failures in microelectronics packages can be traced back to moisture [1,2]. The mechanical behavior of polymer systems is affected significantly by the absorption of atmospheric moisture. Absorbed moisture may lead to plasticization of the material and, thereby, affect the material's mechanical performance. There is an associated reduction in the polymer glass transition temperature, which reduces the maximum allowable operating temperature of material. The softened polymer is also susceptible to swelling and induced damage from the internal vapor pressure developed by the evaporation due to the phase change of moisture at elevated temperatures [3–5]. The rate and quantity of moisture absorbed are both dependent upon the relative humidity, environmental temperature, polymer chemistry, and the mechanisms by which moisture is absorbed [6–8]. Three types of failures arise when an electronic device is exposed to humidity conditions [9]. The first type of failure is often referred to 'popcorn failure' at soldering reflow during rapid heating. The second type of moisture-induced failure mechanism concerns the package reliability during a life-long service period under various field environmental conditions due to swelling-induced damage [10]. The third type is due to electrochemical migration (corrosion) in the presence of both electrical bias and moisture [1]. Dentritic growth and conductive anodic filament (CAF) growth are typical corrosion phenomena observed in high-density substrates. With new polymer systems being developed to meet the requirement of the design and reliability of next generation 3-D system-in-packages, it becomes increasingly important to characterize moisture absorption behavior and understand the material damage induced by moisture transport.

In this paper, several experiments were performed to reveal the fundamental characteristics of moisture behaviors in polymer

* Corresponding author. Address: Department of Mechanical Engineering, P.O. Box 10028, Lamar University, Beaumont, TX 77710, USA. Tel.: +1 409 880 7792; fax: +1 409 880 8121.
E-mail address: xuejun.fan@lamar.edu (X.J. Fan).

0026-2714/$ - see front matter © 2009 Elsevier Ltd. All rights reserved.
doi:10.1016/j.microrel.2009.03.006

systems and the interactions of moisture with polymer matrix. Moisture weight gain tests were carried out for several types of packaging materials. Both Fickian and non-Fickian kinetics of moisture absorption and desorption were investigated. Saturated moisture concentrations at different humidity levels as a function of temperature were measured for two types of materials. A specific experiment was designed to reveal the passage of moisture vapor through a hydrophobic membrane. The difference in water sorption (immersion in water) and moisture sorption (in humid air) was investigated. Mercury intrusion method was introduced to measure the sizes of nano-pores or free-volumes for different types of packaging materials. An approximate method to estimate the free volume fraction is proposed based on moisture weight gain test data. Moiré interferometry technique was applied to study the aging effect of hygroscopic swelling of a polymeric material as a function of time. Finally, a general framework of the governing equations for a deforming polymer with consideration of moisture transport and phase change is presented.

2. Fickian and non-Fickian moisture diffusion

Fickian transport of moisture in polymers or polymer composites is described by

$$\frac{\partial C}{\partial t} = D\left(\frac{\partial^2 C}{\partial x^2} + \frac{\partial^2 C}{\partial y^2} + \frac{\partial^2 C}{\partial z^2}\right) \tag{1}$$

This equation is known as the general diffusion law or Fick's second law of diffusion (Fick's law, for short). C (kg/m^3) is the moisture concentration, t (s) the time, and D (m^2/s) is the diffusion coefficient or diffusivity of the moisture in polymers.

The temperature dependence of the diffusion constant can be described by the Arrhenius equation as follows:

$$D = D_o \exp\left(-\frac{E_d}{kT}\right) \tag{2}$$

where D_o is a pre-factor, E_d is the activation energy, $k = 1.38 \times 10^{-23}$ J/K is the Boltzmann's constant, and T the absolute temperature. It should be noted that the pre-factor and the activation energy constants are different across the glass transition temperature [1]. In other words, there are generally two sets of constants for a material to fully describe the moisture diffusivity as a function of temperature in a range across the glass transition temperature.

If the one-dimensional case of an infinite plate of thickness $2h$ is considered, a general analytical solution, giving the temporal and spatial moisture concentration, C, at time t and distance x from the mid-plane, is described by:

$$\frac{C(x,t) - C_0}{C_i - C_0} = 1 - \frac{4}{\pi}\sum_{n=0}^{\infty}\frac{(-1)^n}{(2n+1)}\exp\left[-\frac{(2n+1)^2\pi^2 D}{h^2}t\right] \cdot \cos\frac{(2n+1)\pi}{h}x \tag{3}$$

With the initial and boundary conditions

$$\begin{aligned} &C = C_0, \quad -h/2 < x < h/2, \quad t = 0 \\ &C = C_i, \quad x = -h/2, x = h/2, \quad t \geq 0 \end{aligned} \tag{4}$$

here C_i is a constant moisture concentration imposed on the boundary, C_0 is the initial moisture concentration, D is the Fickian diffusion coefficient and h is the half-thickness of the plate. When the plate is initially dry and placed into a humid environment, $C_0 = 0$, and $C_i = C_{sat}$ (the saturated moisture concentration), Eq. (3) becomes

$$C(x,t) = C_{sat}\left[1 - \frac{4}{\pi}\sum_{n=0}^{\infty}\frac{(-1)^n}{(2n+1)}\exp\left[-\frac{(2n+1)^2\pi^2 D}{h^2}t\right] \cdot \cos\frac{(2n+1)\pi}{h}x\right] \tag{5}$$

which describes moisture absorption as a function of time. With the time increasing, the plate will be fully saturated with a uniform distribution of moisture concentration C_{sat}. On the other hand, in Eq. (3), when $C_0 = C_{sat}$, and $C_i = 0$, Eq. (3) becomes,

$$C(x,t) = C_{sat}\frac{4}{\pi}\sum_{n=0}^{\infty}\frac{(-1)^n}{(2n+1)}\exp\left[-\frac{(2n+1)^2\pi^2 D}{h^2}t\right] \cdot \cos\frac{(2n+1)\pi}{h}x \tag{6}$$

which describe a desorption process, in which a plate that is initially fully saturated releases moisture in a dry environment. The moisture content in plate will be driven out completely as time goes on.

Since it is not possible to measure the moisture concentration at a point experimentally, Eq. (3) is integrated over the thickness of the bulk plate, and therefore, the total moisture mass of the specimen as a function of time can be obtained as follows:

$$\frac{M_t}{M_\infty} = 1 - \frac{8}{\pi^2}\sum_{n=0}^{\infty}\frac{1}{(2n+1)^2}\exp\left[-\frac{(2n+1)^2\pi^2 D}{h^2}t\right] \quad \text{for moisture absorption} \tag{7}$$

$$\frac{M_t}{M_\infty} = \frac{8}{\pi^2}\sum_{n=0}^{\infty}\frac{1}{(2n+1)^2}\exp\left[-\frac{(2n+1)^2\pi^2 D}{h^2}t\right] \quad \text{for moisture desorption} \tag{8}$$

where M_t is the total mass of moisture at time t, and M_∞ is simply related to C_{sat} by

$$C_{sat} = \frac{M_\infty}{V}, \tag{9}$$

where V is the total volume of the specimen, and M_∞ is the saturated mass of moisture over the plate. When analyzing the experimental data, D and M_∞ are optimized so that the difference between the experimentally determined M_t and the one calculated using Eq. (3) is minimized [11]. Here the change of sample volume caused by moisture absorption–desorption can be ignored since it is quite small (will be discussed later). Both C_{sat} and D are critical in understanding moisture-related reliability issues, because C_{sat} determines moisture absorption capacity, and D determines the rate of diffusion.

It is important to note that in Eq. (1) the diffusivity in Fickian diffusion is assumed to be independent of moisture concentration. While Fick's diffusion model provides a reasonable approximation to the characteristics of moisture uptake, it rarely provides a full description of the uptake data and is unable to account for changes to polymers due to relaxation, degradation, or cracking. Non-Fickian behavior is the consequence of a relaxation process in polymer molecules and/or the result of an irreversible reaction between polymer and moisture such as formation of hydrogen bonds and chemical reactions [12,13]. It has been found that non-Fickian diffusion can take diverse forms [6]. Two-stage or dual-uptake diffusion has been observed in some polymeric materials and is referred as anomalous moisture uptake in the literature (e.g. [6]).

Moisture weight gain measurements are a common experimental technique to evaluate the moisture uptake. In order to investigate the Fickian and non-Fickian moisture absorption kinetics, moisture weight gain measurements were performed for several different materials. The details of specimen geometries and temperature/humidity conditions are as follows:

1. A conventional underfill. The sample is a disk shape with a diameter of 50 mm and a thickness of 1 mm. Moisture absorption under 85 °C/85% RH was performed.
2. A thin bismaleimide-triazine (BT) core material. 7 mm × 7 mm with a thickness of 70 μm. In this study, moisture absorption–desorption experiments were performed at 30, 60, and 80 °C, respectively. At each isothermal temperature, two relative humidity levels were chosen: 60% and 80% RH, respectively. In situ measurement was performed for this thin sample [11].
3. A thick bismaleimide-triazine (BT) core material. The sample size is 50 mm × 50 mm with a thickness of 0.6 mm. Moisture absorption was performed under 30 °C/60% RH.
4. A conventional mold compound: two different sample geometries both from the same material in the form of molded disks were produced with the thickness of 1 mm (MC1) having a diameter of 50 mm and the samples with the thickness 2 mm (MC2) having a diameter of 100 mm, respectively. They were then exposed to the 85 °C/85% RH conditions in a humidity chamber [12].

To determine the dry weights, the samples were dried initially at 125 °C for 24 h. An electronic balance scale was used for the weight gain measurements except for the thin BT core, in which an in situ measurement was performed [11]. The samples were periodically removed and weighed and returned to the chamber for further soaking.

Fig. 1 is a plot of Fickian fit for moisture uptake for an underfill sample compared to the experimental data. To determine the diffusivity D and the saturated weight gain (M_∞), the least-square fitting technique was used. In this approach, the sum of the square of the differences between the experimental weight gain and the calculated one, $(\Delta M)^2 = \sum_{i=1}^{k}(M_{t,i}^{\exp} - M_{t,i}^{cal})^2$, was calculated based on Eq. (7), using some initial estimated values of D and M_∞. $M_{t,i}^{\exp}$ was the ith point of the experimentally determined weight gain at time t, while $M_{t,i}^{cal}$ was the calculated one based on Eq. (7), and k is the total number of experimental points used in calculating $(\Delta M)^2$. Then, D and M_∞ were varied until $(\Delta M)^2$ was minimized. The obtained D and M_∞ are taken as the diffusivity and the saturated moisture mass of the sample for that particular temperature/humidity condition.

From the Fig. 1, it can be seen that the Fick's diffusion law predicts the experimental behavior very well within the tested period. With increasing t, the absorption curve smoothly levels off to a saturation level M_∞. Our previously tested results on different types of underfill also exhibited Fickian behaviors [3].

Fig. 2 shows an example of moisture absorption–desorption experiment for a thin BT core, where the temperature was kept at 60 °C and the RH level was cycled between 0% and 60%. During the first 60 min, a 0% RH condition was imposed to drive any residual moisture out of the sample. This was followed by a 200 min of moisture absorption at 60% RH, then a 200 min desorption at 0% RH.

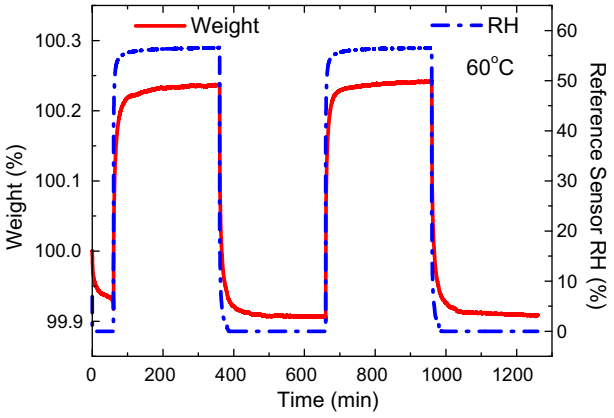

Fig. 2. Moisture absorption–desorption experiment conducted using a sorption TGA at 60 °C with the RH level cycled between 0% and 60% [11].

Based on the results from Fig. 2, several points are clear: (1) during the first 60 min, the moisture was not completely driven out of the sample, a longer time was needed to accomplish that; (2) the subsequent absorption–desorption cycles were repeatable, i.e., the sample reached approximately the same saturated moisture level during sorption and it lost the same weight upon drying. This indicates that there is no chemical reaction between the water molecules and the material. However, as shown in Fig. 3, the Fickican fit is not satisfactory. This might be due to the fact that the BT core has a highly inhomogeneous structure involving glass fibers and resin matrix.

Fig. 4 is a plot of the moisture weight gain for a thick BT core with a thickness of 0.6 mm at 30 °C/60% RH. After the extended hours of moisture absorption, the moisture uptake starts to increase again. It clearly shows the two-stage moisture absorption. The material behaves initially as Fickian's behavior, followed by a non-Fickian diffusion behavior.

The moisture absorption for a mold compound is plotted in Fig. 5 with two different thicknesses. An initial moisture uptake to quasi-equilibrium (the first stage of 'virtual' saturation) is followed by a slower linear moisture uptake. This suggests that at least two different mechanisms are available in the moisture absorption. The first mechanism is the absorption of water

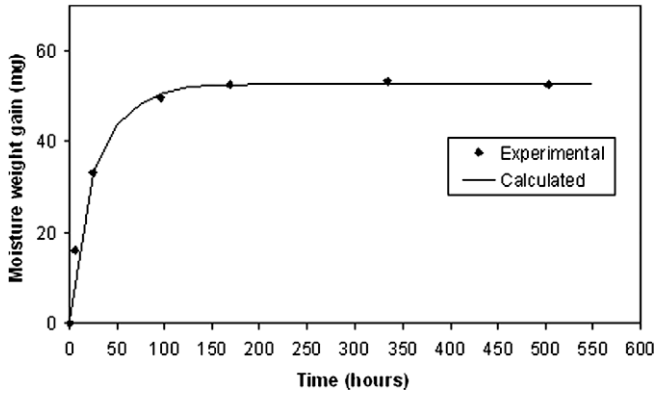

Fig. 1. Fickian curve fit for a homogeneous underfill material under 85 °C/85% RH (sample size 50 mm × 50 mm × 1 mm).

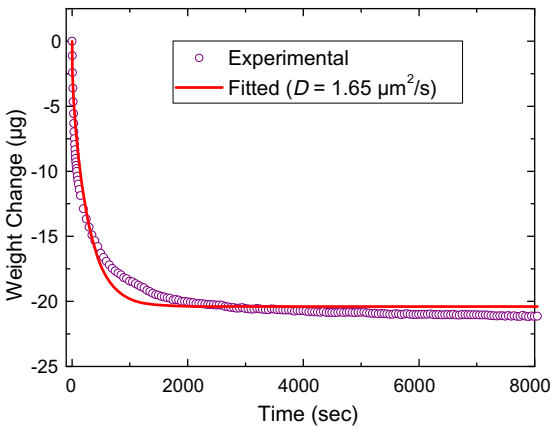

Fig. 3. Desorption curves of a 70 μm BT core. Solid line represents the fitted weight loss versus time curve using $D = 1.65 \times 10^{-8}$ cm²/s by Fick's law [11].

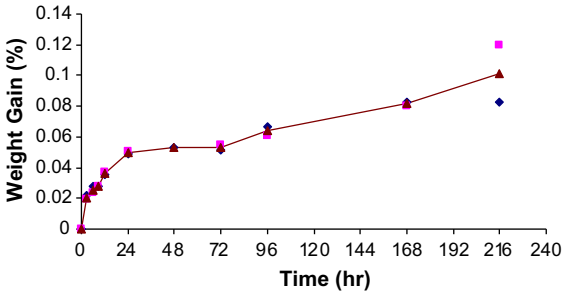

Fig. 4. Moisture weight gain curve for a thick BT core sample with the thickness of 0.6 mm subjected to 30 °C/60% RH.

molecules in free-volumes or nano-voids. The second mechanism is the hydrogen bonding formation between the water molecules and polymer chains due to their molecular polarity. The former mechanism reaches a saturation point and is a reversible phenomenon in nature. The latter seems to be linear without a clear saturation, at least for the time scales reported in this study. The thicker sample (MC2) was further exposed in humid environment for 8 months. The experimental data showed that the moisture weight gain reached about 0.3% after 8 months compared to the 0.2% at the Fickian saturation point. Our latest experimental data showed that about 40% of residual moisture content is not released after a long period of desorption at 110 °C for MC2 [12].

Although the composition and chemistry are different among underfill, BT, and mold compound samples, it has not been clear the mechanisms to cause the difference in moisture uptake between those materials. A mold compound showed a stronger non-Fickian absorption kinetics than an underfill.

Vrentas and Duda [14] introduced a diffusion Deborah Number $(DEB)_D$ to indicate the presence of non-Fickian effects during absorption experiments. There are a number of non-Fickan diffusion kinetics theories [6], of which, the "two-stage" sorption is a frequently encountered non-Fickian type of absorption. The general appearance of the two-stage sorption is characterized by a rapid initial uptake to a quasi-equilibrium, followed by a slower approach to a final, true equilibrium. Ultimately, saturation will be reached for all instances. A theory, satisfactorily describing the features of 'two-stage' sorption, has been proposed by Hopfenberg et al. [15]. In their diffusion relaxation model they considered the absorption process to be composed of two phenomenologically independent contributions: a diffusion part $M_F(t)$ that is governed by Fick's law and a structural part $M_R(t)$, resulting from polymer

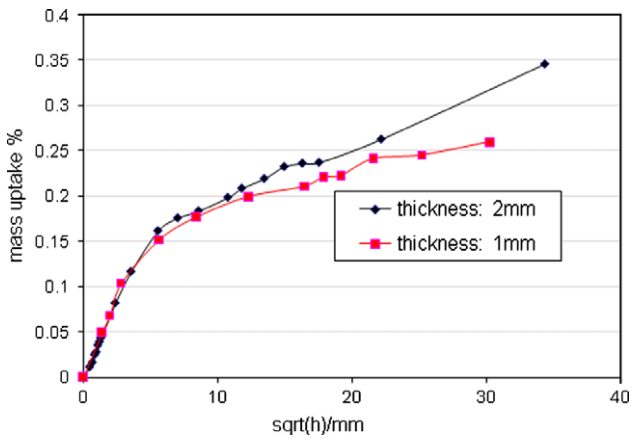

Fig. 5. Normalized moisture uptake of a conventional mold compound with different thicknesses at 85 °C/85% RH (*x*-axis is sqrt(time)/thickness).

relaxations. The total weight gain at time t may be expressed as the linear superposition of these contributions, as follows

$$M(t) = M_F(t) + M_R(t) \tag{10}$$

$M_F(t)$ is given by solutions of the diffusion equation (1). It is assumed that more than one independent relaxation process is possible, so $M_R(t)$ is given by

$$M_R(t) = \sum_i M_{\infty,i}(1 - e^{-k_i t}) \tag{11}$$

where $M_{\infty,i}$ represents the equilibrium absorption due to the ith relaxation process, and k_i is the first-order relaxation constant of the ith relaxation process. It has been shown such a model can describe the non-Fickian behaviors well [6].

Whether the non-Fickian effect should be considered depends on the duration of exposure time to moisture in field or testing conditions. If the exposure time is within the period before polymer relaxation has taken place, Fick's law will describe the moisture diffusion very well. Otherwise non-Fickian's behavior must be accounted for. The duration of moisture exposure required by IPC/JEDEC standards at different humidity levels is usually 7–9 days. To determine the exposure time where Fickian law is valid, moisture diffusion modeling is necessary since the exposure time depends on material's chemistry, geometry and humidity level, and package dimensions.

3. Saturated moisture concentration

Saturated moisture concentration $C_{sat,}$ is a measure of the moisture absorption capacity under given humidity and temperature conditions. According to the definition of the relative humidity

$$\mathrm{RH} = \frac{p}{p_{sat}} = \frac{\text{actural partial water vapor pressure of the air}}{\text{saturated partial water vapor pressure of the air}} \times 100\% \tag{12}$$

the partial water vapor pressure of the air under the given RH and T then is

$$p = \mathrm{RH} \times p_{sat} \tag{13}$$

where p_{sat} is the saturated water partial vapor pressure, which is a function of temperature. Assuming that the Henry's law applies, we have

$$p = \frac{C_{sat}}{S} \tag{14}$$

$$\text{or} \quad S = \frac{C_{sat}}{p} \tag{15}$$

where S is the solubility and a material property, which is independent of the ambient relative humidity. From Eqs. (13) and (15), the following relationship can be obtained

$$C_{sat} = (S \times p_{sat})\, RH \tag{16}$$

Eq. (16) indicates that the solubility can be obtained when C_{sat} is measured at different temperatures. Since the solubility and the saturated water vapor pressure is only function of temperature, according to Eq. (16), the saturated moisture concentration is linearly proportional to the relative humidity if the Henry's law is obeyed. Such a linear relationship is confirmed from a moisture weight gain test for a thin BT sample obtained from a RH step scan experiment, shown in Fig. 6. It reveals that at a fixed temperature (30 °C in this case), C_{sat} is linearly proportional to the RH level.

Fig. 7 plots the saturated moisture concentration in the BT sample as a function of temperature for two different RH levels. These

data were obtained from moisture absorption–desorption experiments. It clearly shows that C_{sat} in BT core is essentially temperature independent.

For most polymer materials at the temperature well below the glass transition temperature, C_{sat} is independent of temperature. This implies that the solubility decreases with temperature according to Eq. (16). However, the situation will be different when the temperature is across the glass transition temperature (T_g). Fig. 8 plots the saturated moisture concentration for a die-attach film as a function of temperature in a range from 30 to 80 °C at 60% RH level. It shows a strong dependency with temperature. This film has a T_g around 35 °C. It reveals that in the temperature region across the T_g, the saturated moisture concentration depends strongly on the temperature. As a matter of fact, since the saturated moisture concentration has strong dependency on the free volume fraction, it is suggested that the saturated moisture concentration will increase significantly when temperature goes across the glass transition temperature. It becomes very important to investigate the saturated moisture concentration at reflow temperature since an 'over-saturation' phenomenon will be observed at the reflow [16,17]. Over-saturation refers to a situation that a material might continue to absorb more moisture despite that desorption takes places during soldering reflow. When saturated moisture concentration is a function of temperature, the moisture diffusion modeling using normalization approach is no longer valid [3]. A direct moisture concentration (DCA) has been proposed to conduct moisture diffusion modeling at reflow process [16,17].

4. Water sorption and moisture sorption

When a polymer material is immersed into water, the sorption process is referred to as water sorption. For a material that is subjected to a humid air condition with a relative humidity less than 100%, it is referred to as moisture sorption process. There are two distinct diffusion mechanisms involved in the transport of moisture: transfers across surface and through bulk, respectively. Moisture diffusion mechanism across surface has not been clear [18]. In order to study the difference for water sorption versus moisture sorption, an experiment of moisture weight gain test and sensitivity/reflow test for two groups of QFN packages was conducted. One group of QFN packages was coated with a hydrophobic membrane, which was formulated by a grafting method [19], to prevent water uptake, while the other group was as received. Two types of moisture preconditioning were applied: immersion into water at a constant temperature of 60 °C, and placement in a humidity chamber at 60 °C/85% RH. Both sorption durations were 192 h. Table 1 summarizes the weight gain test data and the results after the reflow. The coated packages under water did not have any weight change. However, the coated packages in humid air condition gained almost the same amount of moisture compared to the uncoated packages either in water or in humid air. Further, the reflow test indicates that the coated packages at 60 °C/85% RH preconditioning had the same failure rate with the uncoated in the same preconditioning conditions, while the coated packages immersed under water did not show any failures after the reflow. These results imply that a hydrophobic polymer film is very effective in blocking water liquid from penetrating through surface, but not for water vapor transmission (see Fig. 9). Several other hydrophobic polymeric materials have been found to exhibit the similar phenomenon of water vapor passage in humid air conditions [20]. More studies are needed to understand the surface diffusion mechanism. Throughout this paper, unless it is stated, the moisture absorption process is generally assumed.

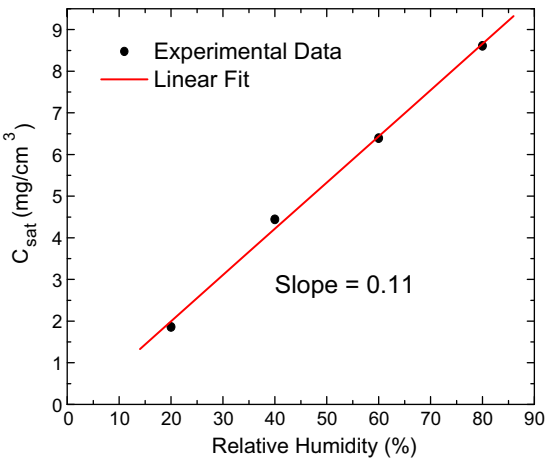

Fig. 6. C_{sat} as a function of relative humidity at 30 °C [11].

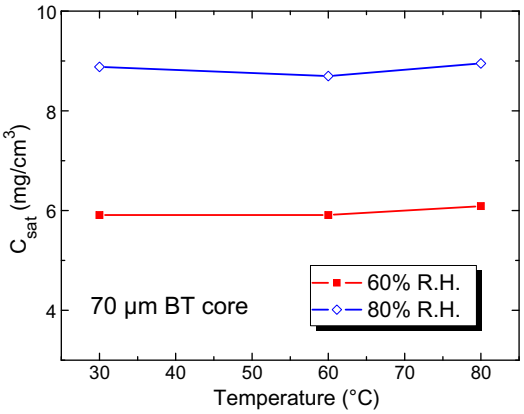

Fig. 7. Saturated moisture content as a function of temperature for two different RH levels [11].

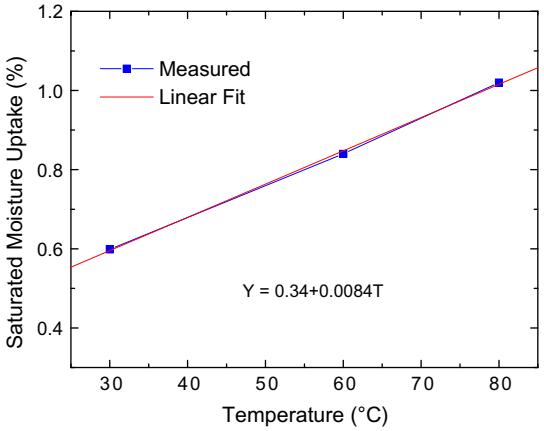

Fig. 8. Saturated moisture concentration as a function of temperature for a die-attach film at 60% RH level (T_g of the film is 35 °C).

5. Characterization of pore size, porosity and free volume

Porosity or free volume fraction of polymers are critical material properties related to moisture absorption. Polymer volume is divided into three elements: occupied volume (the "van der Waals" volume), interstitial free volume, and hole-free volume [21,22]. The hole-free volume is accessible for penetrant transport, and may be altered by absorption and desorption of penetrants.

Table 1
Effect of hydrophobic membrane on moisture sorption versus water sorption.

Sorption condition	Hydrophobic film coated	Weight gain (%)	Reflow test failure rate
Water immersion (60 °C)	Yes	0.03	0/12
Water immersion (60 °C)	No	0.32	7/12
Moisture sorption (60 °C/60% RH)	Yes	0.31	6/12
Moisture sorption (60 °C/60% RH)	No	0.31	8/12

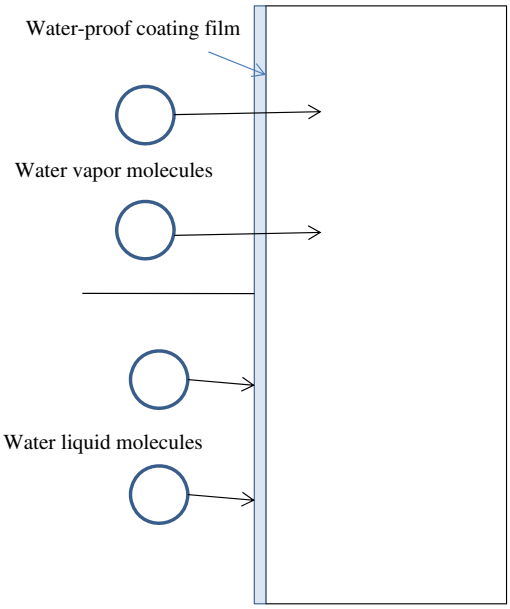

Fig. 9. Schematic diagram for a hydrophobic coating film, which can prevent liquid phase moisture, but not vapor phase moisture, from penetrating into the film.

Changes in the total polymer volume are largely governed by changes in the hole-free volume.

Mercury intrusion porosimetry characterizes a material's porosity by applying various levels of pressure to a sample immersed in mercury [23]. The pressure required to intrude the mercury into sample's pores is inversely proportional to the size of pores. Mercury porosimetry is based on the capillary law governing liquid penetration into small pores. This law, in the case of a non-wetting liquid like mercury, is expressed by the Washburn's equation

$$D = \frac{-4\gamma\cos\theta}{P} \tag{17}$$

where γ is surface tension of mercury, θ is the contact angle between the mercury and the sample, P is the applied pressure, and D is the pore diameter, all in consistent units. The volume of mercury V penetrating the pores is measured directly as a function of applied pressure. This P–V information serves as a unique characterization of pore structure. The Washburn equation assumes that all pores are cylindrical. Although pores or free-volumes are rarely cylindrical in reality, this equation provides a practical representation of pore distributions, yielding very useful results for most applications. As pressure increases during an analysis, pore size is calculated for each pressure point, and the corresponding volume of mercury required to fill these pores is measured. These measurements taken over a range of pressures give the pore volume versus pore size distribution for the sample material. Mercury porosimetry can determine pore size distribution accurately. Comprehensive data provide extensive characterization of sample porosity and density. Available results include total pore volume, pore size distribution and pore diameter. In general, mercury porosimetry is applied over a capillary diameter range from 50 nm to 360 μm.

Several types of polymer materials in packaging applications, such as die-attach films, solder mask, and underfills, were tested using Mercury intrusion [23]. Those materials were also examined for moisture weight gain test at 85 °C/85% RH. The results showed that the relative weight gain ranged from 0.48% to 1.27% for those tested materials. However, no significant pore size down to ~50 nm was observed for all materials. This implies that the free-volumes, which are occupied by the absorbed moisture, are typically in nanometer range. The same materials were then subjected to a simulated reflow process. Fig. 10 shows an example of microstructures of a die-attach film before and after the reflow. It can be seen that the significant voiding of film due to internal vapor pressure was developed after the reflow process [24]. Soles et al. [25] used Positron Annihilation Lifetime Spectroscopy (PALS) to quantify the polymer network topology, which produces a nanovoid volume fraction as a function of temperature. A strong correlation was observed between the absolute zero volume fraction and the ultimate moisture uptake. Although the correlation is clear, the absolute moisture zero hole volume fraction is not sufficient to predict the ultimate moisture uptake.

An approximate estimate method to obtain the free volume fraction of polymers is proposed using moisture weight gain test. Consider a material with a saturated moisture concentration C_{sat} at the given temperature and humidity. If the moisture density in those pores or free-volumes is denoted as ρ within a representative volume element (to be discussed later), the following relationship exists [16]:

$$f_0 = \frac{C_{sat}}{\rho} \tag{18}$$

where f_0 is the initial free volume fraction.

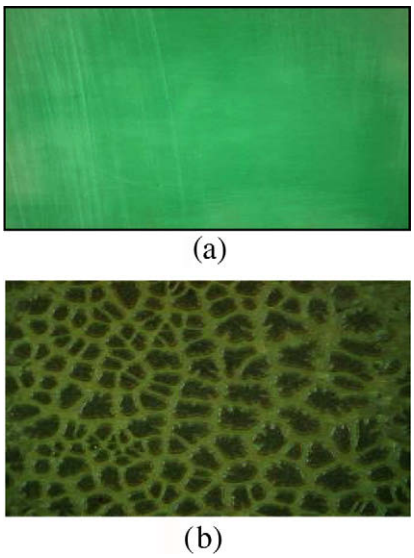

Fig. 10. Microstructures of a soft die-attach film (a) before and (b) after reflow with moisture absorption.

Since the density of the liquid water is1.0 g/cm^3, the moisture density in free volume, i.e., ρ in Eq. (18), must be less than or equal to 1.0 g/cm^3,

$$f_0 \geq C_{sat} \tag{19}$$

when the C_{sat} uses the unit of g/cm^3. In general, the C_{sat} depends on the relative humidity and temperature. It has been suggested that the water liquid will fill in the free volume completely at 100% RH [26,27]. Therefore the initial free volume fraction can be estimated from a moisture weight gain test using C_{sat} measurement data and extrapolated to the 100% RH. This estimate is a low-bound estimation since the moisture will be usually in the mixture of water and vapor in free-volumes. The free volume fraction is usually between 1% and 5% for various packaging materials [28].

6. Hygroscopic swelling measurement

There are a number of experimental techniques for the characterization of hygroscopic swelling of polymers [29–31]. However, few studies have taken the time effect into consideration even though polymers exhibit the viscoelasticity under hygrothermal aging. In this study, silicon/underfill/FR-4 assemblies were prepared as shown in Fig. 11 [10]. The purpose of the study was to investigate the hygroscopic swelling behavior of underfill in a flip-chip assembly-like configuration. The dimensions of the assembly were 8 mm (L) × 5 mm (W) × 1.8 mm (H). The thickness of the underfill was 0.5 mm. A pre-crack was prepared at the silicon/underfill interface, but such a configuration was used for the other purpose of study [10]. In this paper, only the deformation fields at the leftward edge of silicon/underfill interface were reported. An integrated multi-functional micro-moiré interferometry system was developed [10], by combining moiré interferometry (MI) technique with thermoelectric heating and cooling technique (for thermal cycling) and a humidity system (for hygrothermal aging), to investigate the hygroscopic swelling of the underfill. Specimen grating with a frequency of 1200 lines/mm was replicated onto the surface of the assembly at room temperature. The assembly was then put into the miniaturized moisture chamber with the hygrothermal loading conditioned at 85 °C/85% RH for 168 h. The moiré fringe patterns were captured at the times of 0, 1, 3, 7, 11, 24, 48, 96 and 168 h. In order to eliminate thermal effect and investigate the aging effect, a thermal aging test without moisture was carried out on the same assembly and the moiré fringe patterns were acquired at the same time intervals. The aging temperature was kept at 85 °C. The humidity level under the thermal aging test only was 18%, which was expected to cause negligible moisture absorption in the assembly.

The fringe patterns in both x and y-direction at the initial state (t = 0, 85 °C/dry) and different time intervals were presented for the hygrothermal loading at 85 °C/85% RH and thermal loading at 85 °C, in Figs. 12 and 13, respectively. It was observed that the number of fringe orders increased significantly at the beginning. It was believed to be the result of the swelling at the sample surface and the thermal expansion of the underfill material upon moisture absorption and temperature increase. When water immigrated into epoxy-based underfill, it broke the inter-chain bonds by forming hydrogen bonds with chain interruption. The formation of hydrogen bonds permitted the resin network to expand through relaxation of the stresses produced by osmotic pressure. With time going on, the surface portion of the sample was saturated with moisture absorption, and therefore, the increase of fringe orders becomes less significant. The normal strain and shear strain can be extracted from the fringe measurement and were plotted in Fig. 14. The red line represents the strain with moisture uptake. It actually consists of two parts: swelling-induced strain and thermal-mismatch induced strain.[1] The blue line is the experimental results for the same assembly without moisture absorption at a constant temperature of 85 °C. Therefore, the actual swelling-induced strain should be the black line in Fig. 14, which is obtained by the red line subtracted from the blue line. With the consideration of stress relaxation, the actual swelling-induced strains were expected to be greater than those measured in hygrothermal aging. In the Figures, the losses of strains induced by thermal aging were added to the strains measured in hygrothermal aging. As a result, the values of swelling-induced strains were enlarged 20–30%. This implies that the time effect and relaxation due to aging must be taken into consideration to model the swelling behaviors of polymer materials.

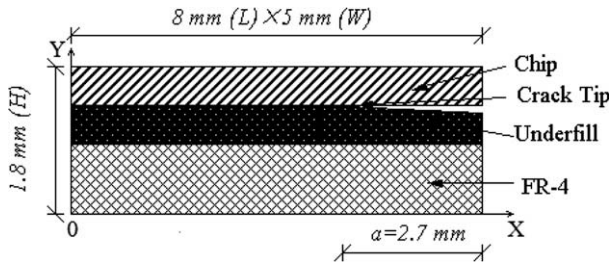

Fig. 11. Schematic diagram of the silicon/underfill/FR-4 assembly.

7. Some discussion

7.1. State of moisture in polymers

When moisture enters the polymer matrix, the moisture is condensed into liquid water phase. For example, let us consider the moisture absorption for an underfill in 85 °C/85% RH condition (moisture absorption data in Fig. 1). Assume that moisture diffusion follows Fickian kinetics with M_∞ being the ultimate moisture weight gain for a sample volume of V. The saturated moisture concentration, C_{sat}, as defined in Eq. (9), can be calculated from a weight gain test. The value of the C_{sat} = 12.5 mg/cm^3. The ambient moisture vapor density at 85 °C/85% RH, i.e., ρ_{ext}, can be obtained from the saturated water vapor density at 85 °C/85% RH

$$\rho_{ext} = 0.85\ \rho_g = 3.04\ e^{-4}\ g/cm^3 \tag{20}$$

where ρ_g is the saturated water vapor density at 85 °C. A simple comparison between the C_{sat} and ρ_{ext} reveal that C_{sat} = 41 ρ_{ext}. If the free volume fraction is 5% of the total sample volume, the actual moisture density in the free volume can be estimated according to Eq. (18) as follows:

$$\rho = \frac{C_{sat}}{f_0} = 820\ \rho_{ext} \tag{21}$$

This implies that the moisture in underfill must be in the binary water liquid/vapor phase. The diffusion process of moisture through polymer systems is a transport process of moisture from ambient vapor phase to the condensed mixed liquid/vapor phase.

Water molecules in polymeric materials have been identified to have two distinct states. "Free" or "unbound" state of water is attributed to water molecules that are present in nano-pores or free-volumes, while "bound" water molecules react with the polymer chains via hydrogen bonding or some chemical reactions [12]. The unbound moisture can be released completely upon a desorption process at the same temperature at which the moisture is absorbed. However, in order to release the bound moisture, more

[1] For interpretation of color in Fig. 14, the reader is referred to the web version of this article.

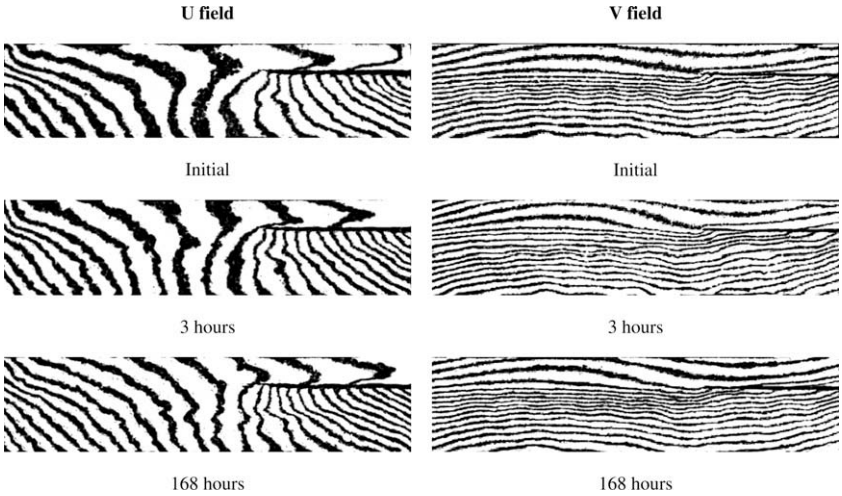

Fig. 12. Fringe patterns during hygrothermal aging under 85 °C/85% RH.

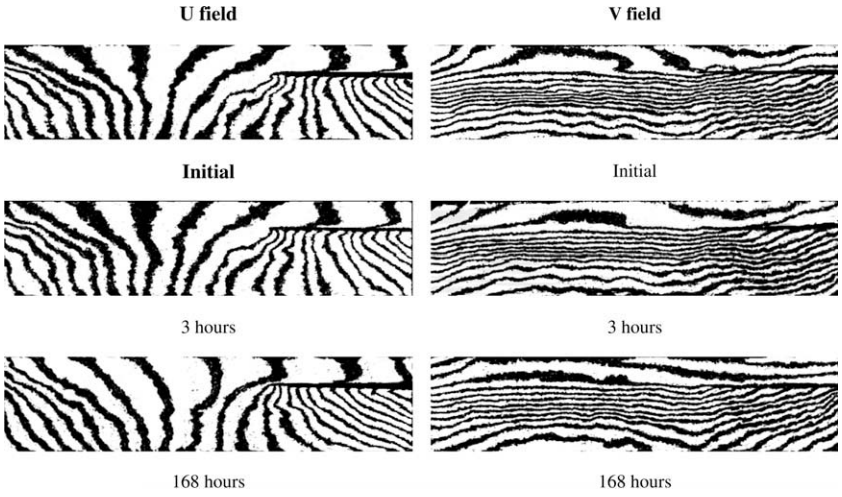

Fig. 13. Representative fringe patterns under the thermal aging test (85 °C).

energy is needed to break the hydrogen bond, and therefore, a higher temperature is needed. Zhou and Lucas [32] studied the mobility of water in different epoxy systems. The study shows that water molecules bind with epoxy resins through hydrogen bonding. Two types of bound water were found in epoxy resins. The binding types are classified as Type I or Type II bonding, depending on difference in the bond complex and activation energy. Type I bonding corresponds to a water molecule which forms a single hydrogen bond with the epoxy resin network. This water molecule possesses a lower activation energy and is easier to remove from the resin. Type II bonding is as a result of a water molecule forming multiple hydrogen bonds with the resin network. This water molecule, therefore, possesses a higher activation energy and is correspondingly harder to remove. Type I bound water is the dominant form of the total amount absorbed water. The amount of Type II bound water depends strongly on the exposure temperature and time. Higher temperature and longer exposure time result in a greater amount of Type II bound water.

7.2. Total moisture volume versus polymer volume expansion

Consider the underfill tested for hygroscopic swelling, the volume change due to hygroscopic swelling based on the test data under 85 °C/85% was determined as [33]

$$\frac{\Delta V}{V} = 0.3\% \tag{22}$$

where V is the total volume of the sample, and ΔV is the volume change due to moisture absorption at a constant temperature.

On the other hand, if the material's free volume fraction is estimated as 3% as a representative value as follows

$$f_0 = \frac{V_{\text{free volume}}}{V} = 3\% \tag{23}$$

It reveals that the volume change by hygroscopic swelling is only a small fraction of the total free volume. In the previous section, the estimate of the free volume fraction does not consider the effect of hygroscopic swelling. This example inferred that the estimate of free volume fraction using weight gain data without considering the material swelling give a good approximation if the material does not swell excessively. Eqs. (22) and (23) indicate that the majority of moisture absorption does not contribute to the material's swelling.

It has been suggested that swelling is caused by water molecules bound to the polymer matrix and not by the free water molecules. Because the water molecule is polar, it is capable of forming hydrogen bonds with hydroxyl groups, thereby disrupting interchain hydrogen bonding with the net effect of increasing the inter-segmental hydrogen bond length. This concept has been

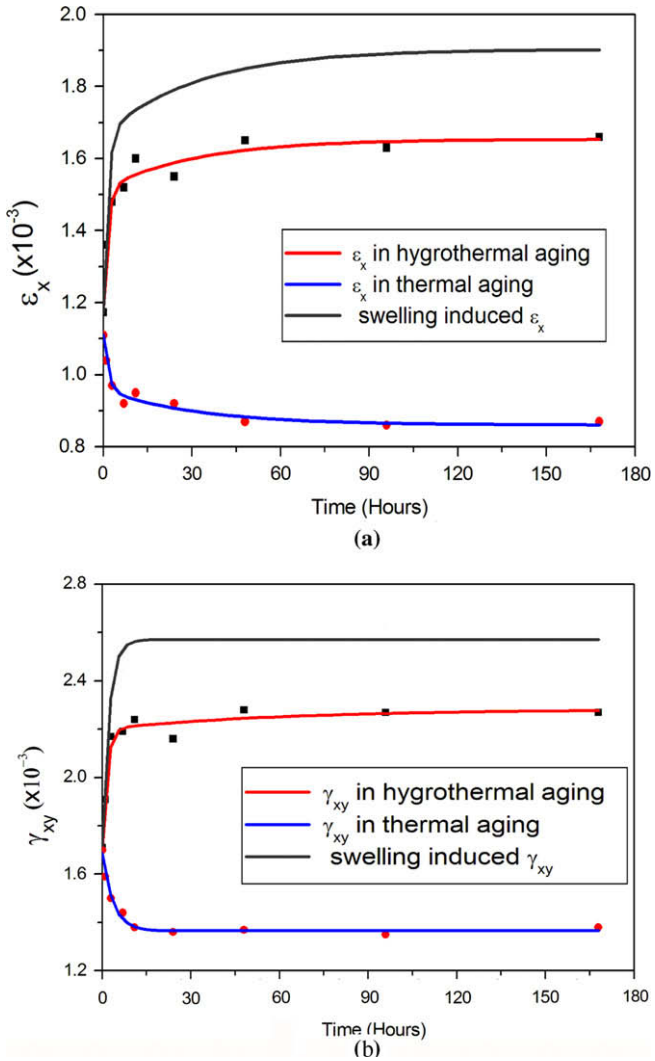

Fig. 14. Swelling induced strains by using superposition method.

observed through spectroscopic methods [34,35]. If such a postulation holds true, the hygroscopic swelling development would include two stages, which correspond to dual-stage moisture absorption theory. In the stage one, the absorption of water molecules take places in free-volumes or nano-voids, which is a reversible process. This stage would not contribute the hygroscopic swelling significantly. In the second stage, the hydrogen bonding is formed between the water molecules and polymer chains, which will cause the material's swelling.

In order to characterize the swelling behavior, the coefficients of hygroscopic swelling (CHS) is often introduced as follows

$$\varepsilon_{\text{swelling}} = \beta C \tag{24}$$

where β is the coefficient of hygroscopic swelling and C is the moisture concentration. According to the above analysis, the formation of hydrogen bond with polymer materials causes the hygroscopic swelling of material, while the unbound water liquid/vapor fills in free-volumes, which does not cause swelling if the vapor pressure is low at lower temperatures. Therefore, the above equation might need to be modified if only a small fraction of moisture is responsible for the swelling of material. Instead of using the total moisture concentration in Eq. (24), the moisture concentration fraction which forms the hygro bonding (Type II) may be used.

$$\varepsilon_{\text{swelling}} = \beta C^{\text{bound water}} \tag{25}$$

where $C^{\text{bound water}}$ is the moisture mass for the bond formation per unit volume.

7.3. Effect of fillers

Many polymer materials used in electronic packaging consist of fillers. While most fillers are not used with the intent of altering the sorption and transport of water within polymer, this concomitant effect is almost always unavoidable. Much of the effect of the fillers on the transport properties within the matrix is governed by the degree of interaction between the polymer matrix and the filler at the interphase. In most composites, it is desirable to have a strong adhesive bond between the two materials. The adhesive bonds can be of either a physical or physicochemical nature. Variations in the strength and nature of these bonds lead to three typical situations at the polymer/filler interface [36].

If the bonds are physical, water can be prevented from reaching the interfacial region and the amount of water absorbed depends only on the epoxy fraction of the composites. If physicochemical bonds, such as hydrogen bonds, are involved, the polymer may find its movement restricted in the vicinity of the filler. If this attraction is strong enough, a portion of the polymer matrix as well as the filler volume may be impermeable to the penetrating moisture.

If poor bonding exists at the interface, water transport may be enhanced by pathways open along the interface. In this case, the water is transported in the liquid state by capillary forces. Similar capillary transport may occur if microcracks and/or defects are present in the bulk of epoxy. Voids at the interface may increase the Langmuir sites of the composites, allowing higher equilibrium sorption. Water clustering in these voids can cause positive deviations from Henry's law [37].

The effect of interfacial bonding can be taken into account by comparing diffusion and sorption in neat polymer resins and composites. If, after correcting for the fiber content of the composite, there is no difference between the two, interphase effects may be negligible. This in general is found for glass/epoxy systems [38].

8. Governing equations for a deforming polymer with moisture considering phase transition

The phenomenological aspect of moisture-induced damage can be found in the works of Fan et al. [39], Hui et al. [40], Roy et al. [41,42], Rajagopal [43], and Sullivan and Stokes [44]. These authors have studied the coupled effect of polymer damage with moisture diffusion. However, a complete mathematical formulation on polymeric solids coupled with the thermodynamics of evaporation of moisture has not been developed. In this section the governing equations for a deforming polymer with moisture are developed. The general case of the moisture phase transition is considered. The governing equations are developed on the lines of soil or rock mechanics with multiphase flow. The solid phase is assumed to comprise a porous skeleton of polymers surrounded by moisture. The moisture flow is neglected here, while an all-round vapor pressure is exerted on the solid phase. The small strain theory is considered here for clarity, but the theory can be extended to large-deformation case. It is assumed that a vapor pressure by moisture, i.e., p, causes only a uniform, volumetric strain by compressing the solids and that the major deformation of the porous skeleton is governed by the effective stress $\boldsymbol{\sigma}'$. This is defined as follows, with the sign convention that tension is positive,

$$\boldsymbol{\sigma} = \boldsymbol{\sigma}' - \mathbf{m}p \tag{26}$$

where $\boldsymbol{\sigma}$ is the total stress and $\mathbf{m}$ is equal to unity for the normal stress components and zero for the shear stress components. At each point in the domain, the variables are in fact average values

over a representative elementary volume (REV) around any considered point in the porous medium domain. As long as the REV is independent of time and of location in the porous medium, the averaged equations obtained are independent of the geometry of the REV. The volume V of a REV is composed by the sum of the volume of solid phase and free volume

$$V = V_s + V_f \tag{27}$$

where V_s is solid phase volume and V_f is the free volume. The (averaged) total stress vector at macroscopic level may be expressed in terms of intrinsic phase averages

$$\begin{aligned}\langle \boldsymbol{\sigma} \rangle &= \frac{1}{V}\int_V \sigma dV = \frac{1}{V}\left[\int_{V_s} \sigma dV + \int_{V_f} \sigma dV\right] \\ &= \frac{V_s}{V}\langle \sigma_s \rangle^s + \frac{V_f}{V}\left[\frac{1}{V_f}\langle \sigma_f \rangle^f\right]\end{aligned} \tag{28}$$

where

$$\langle \sigma_\pi \rangle^\pi = \frac{1}{V_\pi}\int_V \sigma_\pi dV \tag{29}$$

which, presents the average over one-phase. Then we have

$$\langle \boldsymbol{\sigma} \rangle = (1-f)\langle \boldsymbol{\sigma} \rangle^s - f\mathbf{m}\langle p \rangle = \boldsymbol{\sigma}' - \mathbf{m}\langle p \rangle \tag{30}$$

This is how we obtained Eq. (26). For clarity, we do not use the symbol <>, but one should always keep in mind that the quantities are in average at macroscopic level. In Eq. (30),

$$\boldsymbol{\sigma}' = (1-f)(\langle \boldsymbol{\sigma} \rangle^s + \mathbf{m}\langle p \rangle) \tag{31}$$

is the strain-producing stress in the solid skeleton, the effective stress. According to Terzaghi's definition it the sum of the pressure and average stress in the solid phase.

The constitutive equation relating this effective stress to the strains of the skeleton is now independent of the vapor pressure p, and for a general non-linear material can be written in a tangential from, thus allowing plasticity to be incorporated. The expression is written in general from as

$$d\boldsymbol{\sigma}' = \mathbf{D}_\mathbf{T}(d\boldsymbol{\varepsilon} - d\boldsymbol{\varepsilon}_\mathbf{c} - d\boldsymbol{\varepsilon}_\mathbf{p} - d\boldsymbol{\varepsilon}_\mathbf{0}) \tag{32}$$

where $d\varepsilon$ represents the total strain of the skeleton, and represents the overall volumetric strains caused by uniform compression of the particles (as opposed to skeleton) by the pressure of the moisture, with K_s being the bulk modulus of the solid phase. The volumetric strain is relatively insignificant when polymer behaves as rubber where the material is nearly incompressible.

The matrix $\mathbf{D}_\mathrm{T}$ are dependent on the level of effective stresses and also, if strain effects are considered, on the total strain of the skeleton ε. The equilibrium equation relating the total stress to the body forces and the boundary traction specified at the boundary of the domain is formulated in terms of the unknown displacement vector $\mathbf{u}$. When the effective stress relationship is incorporated, the following equation is obtained

$$\begin{aligned}&\int_\Omega \delta\boldsymbol{\varepsilon}^\mathbf{T}\mathbf{D}_\mathbf{T}\frac{\partial \boldsymbol{\varepsilon}}{\partial t}d\Omega - \int_\Omega \delta\boldsymbol{\varepsilon}^\mathbf{T}\mathbf{m}\frac{\partial p}{\partial t}d\Omega + \int_\Omega \delta\boldsymbol{\varepsilon}^\mathbf{T}\mathbf{D}_\mathbf{T}\mathbf{m}\frac{\partial p}{\partial t}\frac{1}{3K_s}d\Omega \\ &- \int_\Omega \delta\boldsymbol{\varepsilon}^\mathbf{T}\mathbf{D}_\mathbf{T}\frac{\partial \boldsymbol{\varepsilon}_0}{\partial t}d\Omega - \int_\Omega \delta\boldsymbol{\varepsilon}^\mathbf{T}\mathbf{D}_\mathbf{T}\frac{\partial \boldsymbol{\varepsilon}_c}{\partial t}d\Omega - \frac{\partial \widehat{\mathbf{f}}}{\partial t} = 0\end{aligned} \tag{33}$$

$$d\widehat{\mathbf{f}} = \int_\Omega \delta\mathbf{u}^\mathbf{T}d\mathbf{b}d\Omega + \int_\Omega \delta\mathbf{u}^\mathbf{T}d\mathbf{t}d\Gamma \tag{34}$$

In order to solve this equation, the vapor pressure evolution model is needed, which was developed in [16,45], as follows:

$$p(T) = \frac{RT}{MM_{H_2O}f}\cdot C, \quad \text{when} \quad C(x,T)/f < \rho_g(T) \tag{35}$$

$$p(T) = p_g(T), \quad \text{when} \quad C(x,T)/f \geq \rho_g(T) \tag{36}$$

where R is the universal gas constant (=8.314 J/(mol · K)), MM_{H2O} is the molecular mass of water (=18 g/mol), C is the local moisture concentration, and p_g is the saturated water vapor pressure. The above expressions have greatly simplified the original vapor pressure model [45], in which three distinct cases are identified to describe the moisture states in pores. The above model does not need to relate the current moisture state to a reference moisture state, but yields exact same results with the original model [16].

In Eq. (33) there are two terms related to the vapor pressure. Previously, the concept of vapor pressure induced expansion was introduced [46]. An integrated vapor pressure, hygroswelling and thermo-mechanical stress modeling methodology during reflow with interfacial fracture mechanics analysis modeling was developed to study the vapor pressure effect [47]. It can be seen that such an effect corresponds to the third term on the left side of Eq. (33). When the material is incompressible, this term vanishes. However, the vapor pressure affects the polymer matrix deformation through the second term, which was not considered in the previous approach.

9. Concluding remarks

Some epoxy-based polymer materials, such as underfill, follow Fick's diffusion law very well on moisture absorption. However, for other materials such as mold compound, non-Fickian behaviors appear significant even within the standard test period. For BT core materials, the absorption-desorption cycles are repeatable, but Fickian fit is not satisfactory. 'Two-stage' sorption theory can describe the non-Fickian diffusion well. The two-stage sorption is characterized by a rapid initial uptake to a quasi-equilibrium state, followed by a slower rate approaching to the final true equilibrium state. For practical reasons, if the attention is focused on the moisture diffusion process when the second stage has not yet taken into effect, the sole Fickian behavior may be applied.

Saturated moisture concentration $C_{sat,}$ is a measure of the moisture absorption capacity under given humidity and temperature conditions. For most polymer materials in microelectronics packaging, C_{sat} does not depend on temperature but RH only as long as the temperature is far below the glass transition temperature. This is an important fact because it provides theoretical foundation for accelerated moisture sensitivity test, in which increasing temperature allows fast moisture absorption but the maximum amount of moisture absorption remains the same. However, the saturated moisture content may increase significantly with temperature when the temperature is across the glass transition temperature.

There are two distinct diffusion mechanisms involved in the transport of moisture: the transfer across the surface and the transfer through bulk. Water sorption appears to be different from the moisture sorption. Hydrophobic film can prevent water liquid molecules from penetrating through the surface. However, this has never been effective for the water vapor transmission through hydrophobic materials.

Pore sizes and porosity (or free volume fraction of polymer) are critical material properties related to the moisture absorption. For most polymer materials, the free volume or pore sizes are in nanometer range though the free volume fraction is usually in the range of 1% to 5%. Significant voiding can be developed at reflow process for soft films.

Moiré interferometry technique was applied to study the aging effect of hygroscopic swelling. It was found that hygroscopic swelling is coupled with stress relaxation. Therefore, a nonlinear viscoelastic model should be used to properly model the polymer swelling behaviors.

The mathematical descriptions of the governing equations for a deforming polymer with moisture effect are presented in this paper.

Acknowledgment

The first author would like to acknowledge many helpful discussions with MIFFT (Moisture-Induced Failure Focus Team) team members at Intel in Chandler, Arizona.

References

[1] Fan XJ. Moisture related reliability in electronic packaging, electronic component technology conference (ECTC) short course notes; 2008.
[2] Zhang GQ, van Driel WD, Fan XJ. Mechanics of microelectronics. Springer; 2006.
[3] Fan XJ, Zhang GQ, van Driel WD, Ernst LJ. Interfacial delamination mechanisms during reflow with moisture preconditioning. IEEE Trans Compon Pack Technol 2008;31(2):252–9.
[4] Lau JH, Lee SWR. Temperature-dependent popcorning analysis of plastic ball grid array package during solder reflow with fracture mechanics method. ASME J Electron Pack 2005;122(1):34–41.
[5] van Driel WD, van Gils MAJ, Fan XJ, Zhang GQ, Ernst LJ. Driving mechanisms of delamination related reliability problems in exposed pad packages. IEEE Trans Compon Pack Technol 2008;31(2):260–8.
[6] Bond DA, Smith PA. Modeling the transport of low-molecular-weight penetrants within polymer matrix composites. Appl Mech Rev 2006;59:249–68.
[7] Galloway JE, Miles BM. Moisture absorption and desorption predictions for plastic ball grid array packages. IEEE Trans Comp Pack Manuf Technol A 1997;20(3):274–9.
[8] Shook R, Conrad T, Sastry V, Steele D. Diffusion model to derate moisture sensitive surface mount IC's for factory use conditions. IEEE Trans Comp Pack Manuf Technol 1996;19(2):110–8.
[9] Fan XJ, Zhou J, Chandra A. Package structural integrity analysis considering moisture. In: Proceedings of electronic components and technology conference (fifty-eight ECTC), p. 1054–66; 2008.
[10] Shi XQ, Zhang YL, Zhou W, Fan XJ. Effect of hygrothermal aging on interfacial reliability of silicon/underfill/FR-4 assembly. IEEE Trans Compon Pack Technol 2008;31(1):94–103.
[11] He Y, Fan XJ. In-situ characterization of moisture absorption and desorption in a thin BT core substrate. In: Proceedings of electronic components and technology conference (ECTC), p. 1375–83; 2007.
[12] Shirangi MH, Fan XJ, Michel B. Mechanism of moisture diffusion, hygroscopic swelling and adhesion degradation in epoxy molding compounds. In: Proceedings of forty-first international symposium on microelectronics (IMAPS), p. 917–23; 2008.
[13] van der Wel GK, Adan OCG. Moisture in organic coatings – a review. Prog Org Coat 1999;37:1–14.
[14] Vrentas JS, Duda JL. Diffusion in polymer-solvent systems II, a predictive theory for the dependence of diffusion coefficients on temperature, concentration and molecular weight. J Polym Sci Polym Phys Ed 1977;15:417–39.
[15] Hopfenberg HB, Stannett VT, Folk GM. Sorption kinetics and equilibriam in annealed glassy polyblends. Polym Eng Sci 1975;15(4):261–7.
[16] Xie B, Fan XJ, Shi XQ, Han D. Direct concentration approach of moisture diffusion and whole field vapor pressure modeling for reflow process: part I – Theory and numerical implementation. ASME J Electron Pack, 2009;131(3):in press.
[17] Xie B, Fan XJ, Shi XQ, Han D. Direct concentration approach of moisture diffusion and whole field vapor pressure modeling for reflow process: part II – Application to 3-D ultra-thin stacked-die chip scale packages. ASME J Electron Pack, 2009;131(3);in press.
[18] Fan XJ. Mechanics of moisture for polymers: fundamental concepts and model study. In: Proceedings of the international conference on thermal and mechanical simulation and experiments in microelectronics and microsystems (EuroSimE), p. 159–72; 2008.
[19] Cui CQ, Fan XJ. Unpublished report on the study of a hydrophobolic coating membrane for preventing moisture-induced failures for QFN packages; 1999.
[20] Personal communications with Mr. Winkler P. of Badger Meter Inc.; 2009.
[21] Tsenoglou CJ, Pavlidou S, Papaspyrides CD. Evaluation of interfacial relaxation due to water absorption in fiber–polymer composites. Compos Sci Technol 2006;66:2855–64.
[22] Webb PA. An introduction to the physical characterization of materials by mercury intrusion porosimetry with emphasis on reduction and presentation of experimental data. Micromeritics Instr Corp 2001.
[23] Koning P, Prack E. Unpublished report on mercury intrusion porosimetry measurement for several kinds of polymer materials; 2006.
[24] Shi XQ, Fan XJ. Wafer-level film selection for stacked-die chip scale packages. In: Proceedings of electronic components and technology conference (fifty-seventh ECTC), p. 1731–736; 2007.
[25] Soles LC, Chang FT, Bolan BA, Hristov HA, Gidley DW, et al. Contributions of the nanovoid structure to the moisture absorption properties of epoxy resins. J Polym Sci: Part B: Polym Phys 1998;36:3035–48.
[26] Fan XJ, Lim TB. Mechanism analysis for moisture-induced failures in IC packages. ASME International Mechanical Engineering Congress and Exposition, IMECE/EPE-14; 1999.
[27] Fan XJ, Zhang GQ, Ernst LJ. A micro-mechanics approach in polymeric material failures in microelectronic packaging. In: Proceedings of third international conference on thermal and mechanical simulation in micro-electronics (EuroSimE), p. 154–64; 2002.
[28] Fan XJ, Zhang GQ, van Driel WD, Ernst LJ. Analytical solution for moisture-induced interface delamination in electronic packaging. In: Proceedings of electronic components and technology conference, p. 733–38; 2003.
[29] Stellrecht E, Han B, Pecht MG. Characterization of hygroscopic swelling behavior of mold compounds and plastic packages. IEEE Trans Compon Pack Technol 2004;27(3):499–505.
[30] Wong EH, Chan KC, Rajoo R, Lim TB. The mechanics and impact of hygroscopic swelling of polymeric materials in electronic packaging. In: Proceedings of fiftieth Electron electronic component technology conference, Las Vegas, NV, p. 576–80; 2000.
[31] Zhou J et al. Effect of non-uniform moisture distribution on the hygroscopic swelling coefficient". IEEE Trans Compon Pack Technol 2008;31(2):269–76.
[32] Zhou J, Lucas JP. Hygrothermal effects of epoxy resin. Part I: The nature of water in epoxy. Polymer 1999;40:5505–12.
[33] Zhang GQ, Fan XJ. Overview: characterization and modeling of moisture behavior of electronic packaging. Micromater Nanomater 2004;3:12–27.
[34] Vanderhart DL, Schen MA, Davis GT. Partitioning of water between voids and the polymer matrix in a polymer compound by proton NMR: the role of larger voids in the phenomena of popcorning and delamination. Int J Microcircuits Electron Pack 1999;22(4).
[35] Toprak C, Agar JN, Falk M. State of water in cellulose acetate membranes. J Chem Soc, Faraday Trans I 1979;75:803.
[36] McMaster MG, Soane DS. Water sorption in epoxy thin films. IEEE Trans Compon Hybrid Manuf Technol 1989;12(3):373–86.
[37] Delasi R, Whiteside JB. Advances composite materials – environmental effects, Vinson JR, editor, ASTM STP-658; 1978.
[38] Mckague EL, Reynolds JD, Halkias JE. Trans Am Soc Mech Eng 1976;98:92.
[39] Fan XJ, Zhou J, Zhang GQ. Multi-physics modeling in virtual prototyping of electronic packages – combined thermal, thermo-mechanical and vapor pressure modeling. J Microelectron Reliab 2004;44:1967–76.
[40] Hui CY, Muralidharan V, Thompson MO. Steam pressure induced in crack-like cavities in moisture saturated polymer matrix composites during rapid heating. Int J Solids Struct 2005;42:1055–72.
[41] Roy S, Xu W. Modeling of diffusion in the presence of damage in polymer matrix composites. Int J Solids Struct 2001;38:115–25.
[42] Roy S, Xu W, Patel S, Case S. Modeling moisture diffusion in the presence of bi-axial damage in polymer matrix composite laminates. Int J Solids Struct 2001;38:7627–41.
[43] Rajagopal KR. Diffusion through polymers undergoing large deformations. Mater Sci Technol 2003;19(9):1175–80.
[44] Sullivan RM, Stokes EH. A model for the effusion of water in carbon phenolic. Compos Mech Mater 1997;26:197–207.
[45] Fan XJ, Zhou J, Zhang GQ, Ernst LJ. A micromechanics based vapor pressure model in electronic packages. ASME J Electron Pack 2005;127(3):262–7.
[46] Tee TY, Fan XJ, Lim TB. Modeling of whole field vapor pressure during reflow for flip chip and wire-bond PGBA Packages. First international workshop on electronic materials & packaging (EMAP), Singapore; 1999.
[47] Tee TY, Zhong ZW. Integrated vapor pressure, hygroswelling and thermo-mechanical stress modeling of QFN package during reflow with interfacial fracture mechanics analysis. Microelectron Reliab 2004;44(1):105–14.